NUKLEONIKA 2014;59(2):53–59
doi: 10.2478/nuka-2014-0011

ORIGINAL PAPER

DE GRUYTER
OPEN

Beta-backscattering thickness-meter design and evaluation with fuzzy TOPSIS method

Afshin Arjhangmehr, Mohammad Mohammadzadeh, Seyed Amir Hossein Feghhi, Saeed Tasouji Hassanpour

Abstract. An industrial gauge for measuring thickness of a gold coating layer deposited on a steel base through detection of the backscattered beta particles has been described. ^{3}H, ^{14}C and ^{63}Ni pure beta emitters have been tested as the radioisotopic sources of the system individually in a fixed geometry. Analytical calculations have been performed in each case. Furthermore, simulations based on Monte Carlo stochastic technique (MCNP) have been processed. The obtained results from both methods have been compared to define the sensitivity of the system in each case. Finally for the first time, fuzzy TOPSIS method has been used for choosing the best source in the defined geometry for manufacturing, considering the following three criteria: (a) saturation thickness, (b) precision and (c) sensitivity. Results have shown that ^{3}H source is the best alternative to the introduced measuring system.

Key words: beta-ray effects • decision making • fuzzy sets • MCNPX

A. Arjhangmehr✉, M. Mohammadzadeh,
S. A. H. Feghhi,
Department of Radiation Application,
Shahid Beheshti University G. C.,
Tehran, Iran,
Tel.: +98 912 439 2064,
E-mail: ms.arjangmehr@gmail.com

S. Tasouji Hassanpour
Department of Industrial Engineering,
K. N. Toosi University of Technology,
Tehran, Iran

Received: 30 October 2013
Accepted: 8 May 2014

Introduction

Mostly, sealed radioactive sources are used in industrial radiography, gauging applications and mineral analysis. Modern industry uses radioisotopes to improve productivity and to gain information that cannot be obtained with other methods.

Measuring thickness of a coating component deposited on a base material through detection of the backscattered beta particles is a conventional non-destructive method that has been well adapted and widely utilized in many industrial applications [1]. In this process, when the intensity of radiation from a radioisotope is being reduced by matter in the beam, a fraction of the radiation is scattered back toward the radiation source. The amount of 'backscattered' radiation is related to the amount of material in the beam, and this can be used to measure characteristics of the material. This principle is used to measure different types of coating thicknesses. Machines which manufacture plastic films use radioisotope gauging with beta particles to measure the thickness of the plastic films [2]. In addition, beta gauges are used in paper manufacturing to monitor the thickness of the products [3]. This type of nuclear gauges provides the opportunity to measure thickness in the scale of several nanometers and they can be easily manipulated. The coating thickness gauges are particularly suitable for quality control in the process of anodising or galvanising, and are essential for measuring coatings in the automotive sectors [4]. This type of gauges has found wide applicability as wall thickness metres that determine the hardness of metal, plastic and glass walls and windows [5].

Besides nuclear gauging, other methods such as ultrasonic and magnetic laser techniques have also proved to be applicable in measuring coatings [6, 7], but the eventual higher accuracy, lower costs and fast timing of the nuclear gauges (especially systems based on beta-backscattering) make them more preferable in high-tech industrial applications.

The backscattering probability of the beta particles primarily depends on the electron density, which directly correlated with: (a) the atomic number and (b) the mass density of the target matter. Experiments have shown that the intensity of the backscattered radiation is depended on the thickness of the coating layer and its saturation value is proportional to the atomic number of the coating component [8]. In this paper, an industrial gauge for measuring thickness of a gold layer (as a high Z component) coated on a steel substrate (as a low Z one) has been outlined and it will be constructed in the Radiation Application Department of the Shahid Beheshti University in a near future. ^{3}H, ^{14}C and ^{63}Ni have been used individually as the beta emitters. Rectangular methodology, which increases the activity by means of implementing three completely separate isotropic sources has been introduced and developed. This method improves the geometry factor of source-to-coating layer and coating layer-to-detector. Geometry factor has a direct correlation with the absolute efficiency of the detector and the obtained pulse height. Silicon lithium (Si(Li)) drifted with respect to its relatively high counting efficiency has been selected as the detector of the measuring system. The detector's active volume thickness is kept quite large, and it is functioning in fully depleted mode.

Because published experimental reports were not available for this type of thickness metres, the analytical and numerical calculations (Monte Carlo) have been performed and compared to determine the validity of the design.

In addition, for the first time, with respect to crisp numbers (definite sets), the fuzzy TOPSIS method has been used for choosing the best beta emitting source, considering the three important criteria: (a) saturation thickness, (b) precision and (c) sensitivity. This method has been employed for enhancing the validity of the radioisotope selection [9, 10]. Moreover, the half-life of the source which determines the effective operational lifetime of the designed system and the maximum energy of emitted particles that defines the effective dose and limits the daily allowed measurement time are other important criteria that should be considered in fuzzy TOPSIS method for advance evaluations. In conclusion, the best configuration based on the results has been selected.

Theoretical computation

Backscattering process

Beta particle incident on the coating layer would interacts primarily with the orbital electrons and because of equal mass, a large fraction of its kinetic energy could be transferred in a single collision. Absorption of the beta particles over a limited region varies exponentially with the thin layer thickness [11, 12]. Because n of the incidents particles can pass the absorber, the intensity of the attenuated and backscattered radiation could be deduced as follow:

$$n = n_0(1-e^{-\mu_m t_d}) \tag{1}$$

$$n_{bs} = p_1 n_1(1-e^{-\mu_m t_d}) \tag{2}$$

where n_0 is the number of the primary incident particles, n is the number of particles that pass the thin absorber, μ_m is the mass attenuation coefficient of the target layer, t_d is its density thickness and p_1 is the probability of the backscattering, which has a direct correlation with Z of the absorber and is independent of the energy of incident radiation [8, 13]. For measuring thickness of a coating component deposited on base material with different atomic numbers, a theoretical equation has already been developed [14].

$$n_{bs} = n_A + n_B = p_1 n_0(1-e^{-\mu_m t_d}) + p_2 n_0 e^{-(\mu_{m1}+\mu_{m2})t_d} \tag{3}$$

where n_{bs} is the total intensity of the backscattered beta particles, p_1 and p_2 are the backscattering probabilities and μ_{m1} and μ_{m2} are the mass attenuation coefficients of the coating and base components, respectively. To have more precise prediction, it is better to consider the spatial position of the coating layer and the semiconductor detector, because detection of all the backscattered particles is not practical.

$$n'_{bs} = \left(\frac{\Omega_d}{2\pi}\right) n_{bs} \tag{4}$$

where Ω_d is the solid angle covered by the detector relative to coating substrate. It has been proved that the saturation thickness, the maximum thickness that could be measured with the outlined radioisotopic gauge is one fifth of the maximum range of beta particles, which can be calculated through the empirical formula introduced by Cember [14]. Upper and lower limits of the response curve is obtained through variation of the coating layer density thickness from zero (no coating layer) to saturation value (t_{sat}), while the thickness of the steel substrate is assumed to be constant and much thicker than the maximum range of beta particles

(a) $t_d = 0$ then $n_{bs} = p_2 n_0 = n_1$,
(b) $t_d = t_{sat}$ then $n_{bs} = p_1 n_0 = n_2$.

Because $Z_{\text{gold}} > Z_{\text{steel}}$ and $p_1 > p_2$, it can be concluded that $n_2 > n_1$ and the predicted response should be an exponential curve. The intensity of the backscattered radiation is extremely dependent over values of the mass attenuation coefficients. Several measurements on mass attenuation coefficients and range-energy relation of β^+ and β^- particles for various absorbers in a wide range of energies have been reported [11, 15]. Baltakment and Thummel had introduced attenuation formula based on available experimental data with an acceptable accuracy [11, 16]. Based on maximum energy and half-life of the available isotopic pure beta emitters, favourite options are ^{3}H, ^{14}C and ^{63}Ni. The important characteristics of the proposed system is acquired in each case and summarised in Table 1. Using Eq. (3) and Table 1, the response curves could be approximated and visualised in each case, the results are shown in Fig. 1.

Table 1. Characteristics derivation

Source	E_m (MeV)	$T_{1/2}$ (year)	t_{sat} (μm)	μ_{m1} ($\times 10^3$)	μ_{m2} ($\times 10^3$)
^{3}H	0.019	12.26	0.174	9.41	7.52
^{14}C	0.156	5730	3.367	0.41	0.33
^{63}Ni	0.067	92	1.037	1.45	1.16

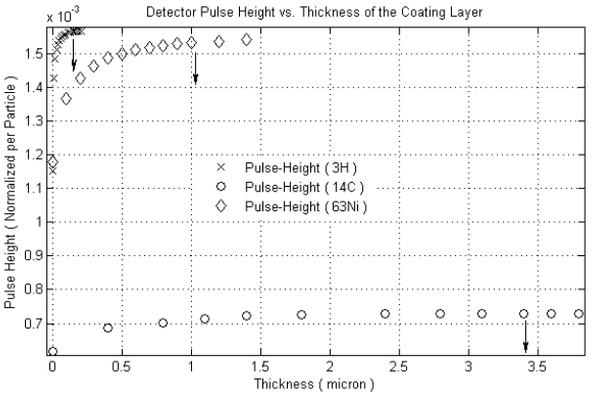

Fig. 1. Normalised response curves obtained from analytical computation of the beta particles scattering backward.

Geometry and efficiency calculation

Because of required high counting efficiency, Si(Li) semiconductor detector have been selected. It has a planar geometry, d = 18 cm in diameter and g = 1 cm in height, with a very thin entrance window, which has negligible effect and the corresponding loss can be neglected. It is fully depleted and operates in current mode. In order to reduce the effect of the background radiation and improve SNR, it has been shielded with lead and concrete pair layers. The detector-to-source and source-to-coating layer spacing are e = 1.6 cm and c = 1 cm, respectively. Diameter of the steel substrate is b = 9 cm. Beta emitters are shielded with a low Z component such as aluminium to diminish the intensity of produced secondary Bremsstrahlung X-rays. Radius of the ring-type beta emitters are considered to be 1 mm (a = 1 mm). The scheme of the system is shown in Fig. 2. With the above mentioned dimensions, and neglecting the effect of the entrance window, all the incident particles on its active volume will be measured as detectable pulses. So, $\varepsilon_{int} \sim 1$ would be a true assumption for the Si(Li) semiconductor detector in the proposed system. A new technique, using three ring-type beta emitters in the crests of a triangle has been developed. This method increases the available activity and improves the absolute efficiency. Described configuration is shown in

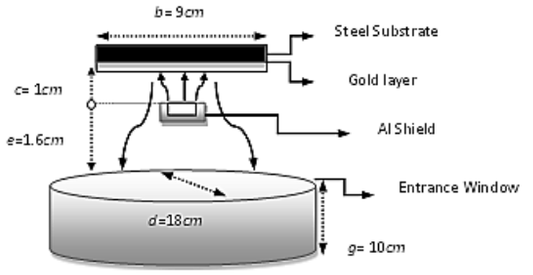

Fig. 2. Schematic of the designed system.

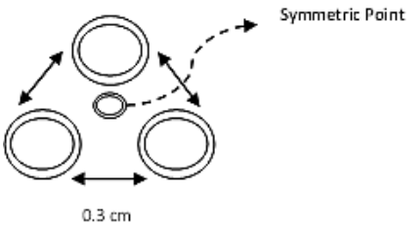

Fig. 3. Triangle source configuration.

Fig. 3. Exact calculation of the absolute efficiency (ε_{abs}) requires measuring the geometry factor (G) and the source-to-coating layer and coating layer-to-detector relative spatial positions.

$$(5) \qquad \varepsilon_{abs} = G \times \varepsilon_{\text{int}} \quad \text{where} \quad G = \frac{\Omega_d}{2\pi} \times \frac{\Omega_s}{4\pi}$$

where Ω is the solid angle covered by the detector in 4π space. In order to simplify the mathematical calculations of the geometry factor, the defined configuration is approximated with a single ring-type source in the middle of the circum – centre (the centre of a circle passing through the three vertices of the triangle as shown in Fig. 3) [17]. The attenuation of electrons in air has not been considered and the calculated mathematical expressions for geometry factors (Ω/4π), corresponding to source-to-coating layer (s) and coating layer-to-detector (d) are as follow:

$$(6) \qquad \frac{\Omega_s}{4\pi} = 0.5\left[1-\left(1+\frac{\left(\frac{b}{2}\right)^2}{c^2\left(1+\frac{a^2}{c^2}\right)^{3/2}}\right)^{-1/2}\right],$$

$$\frac{\Omega_d}{4\pi} = 0.5\left[1-\frac{1}{(1+\xi)^{1/2}}-\frac{3\xi\Psi}{8(1+\xi)^{5/2}} +\Psi^2\left(\frac{5\xi}{16(1+\xi)^{7/2}}-\frac{35\xi^2}{64(1+\xi)^{9/2}}\right)\right]$$

where $$\xi = \frac{\left(\frac{d}{2}\right)^2}{(e+c)^2}, \quad \Psi = \frac{\left(\frac{b}{2}\right)^2}{(e+c)^2}.$$

Expression introduced for calculation of ($\Omega_d/4\pi$) is multiplied by a factor of two, because the solid angle covered by the detector relative to coating layer is in 2π space. Substituting the numerical values, $\Omega_s/4\pi$ = 0.3908, $\Omega_d/2\pi$ = 0.6976 and G = 0.2726 and the predicted value of the absolute efficiency can be calculated using Eq. (5) and is equal to 27.26%. It could be concluded that with the described technique, the absolute efficiency will improve considerably. This technique provides a unique possibility to construct thin sources, which decreases the self-absorption and increases the effective activity.

Simulation based on Monte Carlo stochastic technique

Electron backscattering has been extensively studied in an experimental or theoretical way. Everhart [18]

described the behaviour of backscattered electrons of low energies based on a single elastic scatter collision assumption. Also Archard [19] developed a theory based on the complete diffusion of electrons. Monte Carlo stochastic technique (MCNPX) [20, 21] have been used to evaluate the response of the designed system. All obtained results are normalised per source particle and the procedure has been repeated over 10 million times, in order to reduce the corresponding statistical error. Results of Monte Carlo simulations (F8 tally in MCNPX module) and analytical calculations for ^{3}H, ^{14}C and ^{63}Ni sources are demonstrated and compared in Fig. 4a–c, respectively. It is obvious that there is a small difference (less than 4.5%), which arises from the defined non-ideal (considering air contamination; a non--prefect vacuum between the source and the detector) environment in simulation phase. Also, p_1 and p_2, the

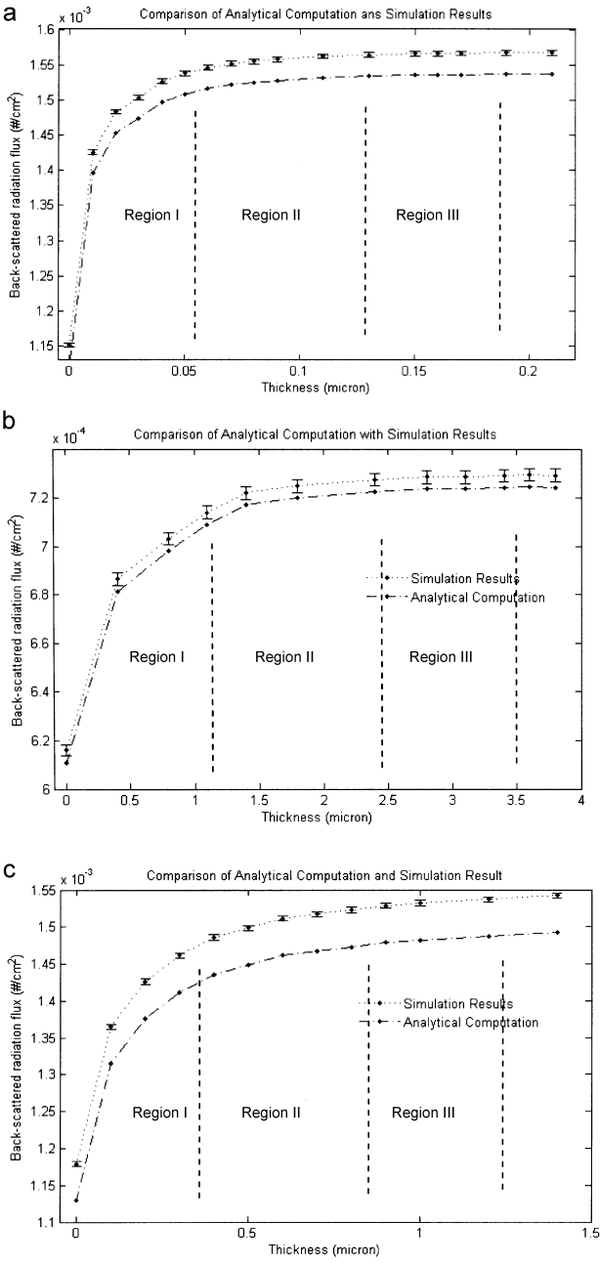

Fig. 4. Comparison of the Monte Carlo simulation results and analytical calculations in each case: (a) ^{3}H, (b) ^{14}C, (c) ^{63}Ni.

Table 2. Backscattering probabilities

	p_1 (%)	p_2 (%)	Beta end-point energy (MeV)
^{3}H	0.574	0.423	0.019
^{14}C	0.268	0.226	0.156
^{63}Ni	0.566	0.433	0.067

radiated beta particles backscattering probabilities from gold and steel substrates have been calculated through application of Monte Carlo stochastic technique and numerical values have been listed in Table 2. Employing Eq. (5) and Table 1, intensity of the backscattered radiation can be predicted analytically in each case. Also, the angular distribution of the backscattered radiation, near the detector's active volume have been computed using MCNPX and shown in Fig. 5a. Large fraction (≈30%) of the backscattered particles is in the range of –25° to +25°. So, in order to surpass the pulse height and improve the SNR, the detector and the source blocks should be set in a straight line. The angle between the surface normal and the particle trajectory is defined as the scattering angle (θ) and has been exhibited in Fig. 5b. Sensitivity is expressed as the pulse-height (PH) variation over the measurable thickness (t_{sat}) and its mathematical relation is as follow:

$$S = \frac{\mathrm{PH}}{t_{sat}}\left(\frac{\mathrm{cps}}{\mu\mathrm{m}}\right) \tag{7}$$

An exact analysis of the obtained results (Table 3) revealed that the sensitivity over small variations of coating thickness in the case of ^{3}H is in an acceptable range and literally is of hundredths of a micrometre. Also, ^{3}H is in high priority, when applications with an accuracy range of several tens of nanometre are required. Beta-rays attenuation with the defined spacing and the introduced geometry is negligible and neither self-absorption, nor particle loss through air contamination should cause a significant difference between simulation and eventual experimental results.

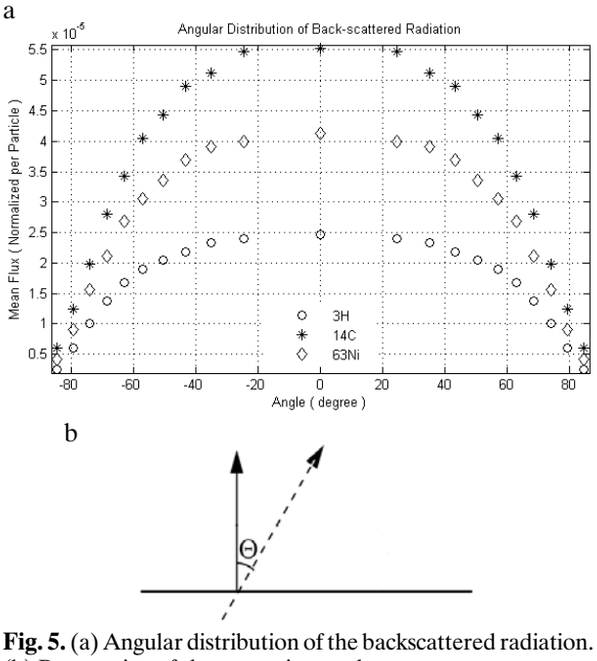

Fig. 5. (a) Angular distribution of the backscattered radiation. (b) Perspective of the scattering angle.

Table 3. Formulised simulation results

	Accuracy range	Sensitivity (%) (cps/μm)			
		Overall	Region I	Region II	Region III
^{3}H	Hundredth of micrometre	2.4564	5.2302	0.7121	0.0598
^{14}C	Tenth of micrometre	0.0033	0.0056	0.0009	0.0001
^{63}Ni	Tenth of micrometre	0.0367	0.0695	0.0098	0.0009

Validation of the results using the fuzzy TOPSIS method

In this section, fuzzy TOPSIS method has been used for enhancing the validity of the radioisotope selection. Because several parameters are effective on the system behaviour, and eventually can change the course of construction, it seems essential to pre-validate gauge important features. The saturation thickness, precision, sensitivity, half-life of radioisotope, and the maximum emitted energy per particle are the characteristics of the designed coating gauge that should be validated based on their values. In previous sections, the 'saturated thickness', the 'precision' of the results and the 'sensitivity' of the gauge in different regions were calculated analytically. These parameters will be analysed based on multi-criteria decision-making (MCDM) method to improve the validity of the radioisotope selection. In the following sections, 'sensitivity', 'precision' and 'saturation thickness', are considered as criteria and ^{3}H, ^{14}C and ^{63}Ni are defined as alternatives.

MCDM refers to screening, prioritising, ranking or selecting a set of alternatives under usually independent, incommensurate or conflicting attributes [22]. Technique for order preference by similarity to ideal solution (TOPSIS) is one the MCDM techniques which is based upon goal aspiration and reference levels. In TOPSIS method two ideal solutions are defined as positive-ideal solution (PIS) and negative-ideal solution (NIS). The goal is to choose the alternative which has the shortest distance from the PIS and the farthest from the NIS. Considering the uncertainty of the real world and the very small scale of the data about alternatives which makes the selection process very difficult, it was determined to use linguistic variables and fuzzy TOPSIS to make the selection become much more precise and close to real world. The concept of linguistic variable is very useful in dealing with situations which are too ill-defined to be reasonably described in conventional quantitative expressions [23, 24]. The ratings of the attributes (criteria) are considered as linguistic variables. The linguistic variables that are defined by the experts can be converted into triangle fuzzy numbers [23–25]. The fuzzy TOPSIS method can be described briefly as follow [9, 10].

First step is to determine the experts to ask them about their ideas about which linguistic variable matches the criteria with respect to each alternative considering the data available. Assume that A_1, A_2 and A_3 represent, respectively, for ^{3}H, ^{14}C and ^{63}Ni sources. Using the linguistic variables shown in Tables 4 and 5, the alternatives will be assessed with respect to decision makers. The matrix format of kth decision maker can be shown in the following format:

$$(8)\quad D^k = \left[f_{ij}^k \right]_{m\times n},\ k = 1,2,...,K;\ i = 1,2,...,m;\ j = 1,2,...,n$$

where f_{ij} is a linguistic variable representing the rating of the ith alternative with respect to jth criteria. These linguistic variables are listed in Table 4 in the format of triangular fuzzy numbers. In order to make the decision matrix unit-free, normalisation approach should be implemented. The process of normalisation is developed in this order: Assume that R^k is the normalised matrix for the kth decision maker.

$$(9)\quad R^k = \left[r_{ij}^k \right]_{m\times n},\ k = 1,2,...,K;\ i = 1,2,...,m;\ j = 1,2,...,n$$

where r_{ij} is the normalised format of $f^k_{ij} = (a_{ij}, b_{ij}, c_{ij})$, which is calculated by means of the following equations: $r^k_{ij} = \{(a_{ij}/c^*_j), (b_{ij}/c^*_j), (c_{ij}/c^*_j)\}$, where c^*_{ij}, stands for maximum value of c_{ij}.

In next step, the relative importance of each attribute (criteria) should be established. There are different methods to do this step such as pair-wise comparisons or obtaining these values directly. In this paper we will use linguistic variables which will be determined by means of the decision maker. These variables are listed in the Table 5. Considering these linguistic variables and the fuzzy value assigned to each criteria, the weighted normalised decision matrix will be obtained as follow:

$$(10)\quad V^k = \left[v_{ij}^k \right]_{m\times n},\ k = 1,2,...,K;\ i = 1,2,...,m;\ j = 1,2,...,n$$

where $v^k_{ij} = r^k_{ij}(x)w^k_j$ and also $v^k_{ij} = (v_{ij1}, v_{ij2}, v_{ij3})$ which represents for weighted normalised of the ith alternative with respect to jth criteria and the kth decision maker. The importance weights of criteria defined by two decision makers are shown in Table 6. In Table 7, the ratings

Table 4. Linguistic variables for rating

Linguistic variables	Triangular fuzzy numbers
Very low (VL)	(0, 0, 1)
Low (L)	(0, 1, 3)
Medium low (ML)	(1, 3, 5)
Medium (M)	(3, 5, 7)
Medium high (MH)	(5, 7, 9)
High (H)	(7, 9, 10)
Very high (VH)	(9, 10, 10)

Table 5. Linguistic variables for the important weight of each attribute

Linguistic variables	Triangular fuzzy numbers
Very poor/very low (VL)	(0, 0, 0.1)
Poor/low (L)	(0, 0.1, 0.3)
Medium poor/medium low (ML)	(0.1, 0.3, 0.5)
Fair/medium (F)	(0.3, 0.5, 0.7)
Medium good/medium high (MH)	(0.5, 0.7, 0.9)
Good/high (H)	(0.7, 0.9, 1)
Very good/very high (VH)	(0.9, 1, 1)

Table 6. Importance weight of criteria from decision makers

	DM1	DM2
C1	H	M
C2	VH	H
C3	H	H

Table 7. Rating for each alternative against each criteria

		C1	C2	C3
DM1	A1	H	VH	VH
	A2	M	VH	H
	A3	MH	VH	VH
DM2	A1	H	H	H
	A2	M	H	H
	A3	MH	H	VH

Table 8. Decision matrix

		C1	C2	C3
DM1	A1	(0.7, 0.9, 1)	(0.9, 1, 1)	(0.9, 1, 1)
	A2	(0.3, 0.5, 0.7)	(0.9, 1, 1)	(0.7, 0.9, 1)
	A3	(0.5, 0.7, 0.9)	(0.9, 1, 1)	(0.9, 1, 1)
DM2	A1	(0.7, 0.9, 1)	(0.7, 0.9, 1)	(0.7, 0.9, 1)
	A2	(0.3, 0.5, 0.7)	(0.7, 0.9, 1)	(0.7, 0.9, 1)
	A3	(0.5, 0.7, 0.9)	(0.7, 0.9, 1)	(0.9, 1, 1)

Table 9. The weighted normalised decision matrix

		C1	C2	C3
DM1	A1	(0. 49, 0.81, 1)	(0.81, 1, 1)	(0.63, 0.9, 1)
	A2	(0.21, 0.45, 0.7)	(0.81, 1, 1)	(0.49, 0.81, 1)
	A3	(0.35, 0.63, 0.9)	(0.81, 1, 1)	(0.63, 0.9, 1)
DM2	A1	(0.21, 0.45, 0.7)	(0.49, 0.81, 1)	(0.49, 0.81, 1)
	A2	(0.09, 0.25, 0.49)	(0.49, 0.81, 1)	(0.49, 0.81, 1)
	A3	(0.15, 0.35, 0.63)	(0.49, 0.81, 1)	(0.63, 0.9, 1)

for each alternative against each criteria with respect to the decision makers are listed. The linguistic matrix shown in Table 7 should be converted into weighted normalised fuzzy numbers. The procedure is shown in Tables 8 and 9. In Table 8 the linguistic variables are replaced with triangular fuzzy numbers and Table 9 consists of weighted normalised fuzzy numbers.

After calculating the weighted matrix, the fuzzy positive ideal solution (FPIS) and the fuzzy negative ideal solution (FNIS) are calculated as distance indexes using following equations:

$$\text{FPIS} = (v_1^+, v_2^+, ..., v_n^+) \tag{11}$$

$$\text{FPIS} = (v_1^-, v_2^-, ..., v_n^-) \tag{12}$$

where v_1^+ and v_1^-, respectively stand for max(v_{ij3}) and min(v_{ij1}) for $i = 1, 2,\ldots, m; j = 1, 2,\ldots, n$. Table 10 illustrates the distance from PIS and NIS for each decision maker. The distance of each alternative with respect to kth decision maker can be calculated as following:

$$d_i^{k+} = \sum_{j=1}^{n} d\left(v_{ij}^k, v_j^+\right), \quad i = 1, 2, ..., m; \quad j = 1, 2, ..., n \tag{13}$$

Table 10. The distance measurement

	DM1		DM2	
	d_i^+	d_i^-	d_i^+	d_i^-
A1	0.64	1.13	0.31	0.34
A2	1.00	0.81	1.08	0.94
A3	0.77	1.01	0.91	1.08

Table 11. Geometric mean value of distance

	DM1	DM2
	d_i^+	d_i^-
A1	0.445421	0.619839
A2	1.039230	0.872582
A3	0.837078	1.044414

Table 12. The closeness index

	C_I^-
A1	0.58
A2	0.46
A3	0.55

$$d_i^{k+} = \sum_{j=1}^{n} d\left(v_{ij}^k, v_j^-\right), \quad i = 1, 2, ..., m; \quad j = 1, 2, ..., n \tag{14}$$

where $d(\mathrm{A}_1, \mathrm{A}_2)$ in which $\mathrm{A}_1 = (a_1, b_1, c_1)$ and $\mathrm{A}_2 = (a_2, b_2, c_2)$ are triangular fuzzy numbers is calculated by the following equation:

$$d(\mathrm{A}_1, \mathrm{A}_2) = \sqrt{\frac{1}{3}\left[(a_1 - a_2)^2 + (b_1 - b_2)^2 + (c_1 - c_2)^2\right]} \tag{15}$$

To integrate the multiple decision-maker approach into a single distance measure for each alternative, the geometric mean will be employed as follows:

$$d_T^+ = \left(\prod_{k=1}^{K} d_i^{k+}\right)^{\frac{1}{k_i}} = 1, 2, ..., m \tag{16}$$

$$d_T^- = \left(\prod_{k=1}^{K} d_i^{k-}\right)^{\frac{1}{k_i}} = 1, 2, ..., m \tag{17}$$

After calculating the overall separation measure by using above equations which is shown in Table 11, the relative closeness for each alternative will be defined as: $C_i^- = [d_T^-/(d_T^- + d_T^+)]$, where $0 \le C_i^- \le 1$. The alternative which has the greater value of C_i^- is the best solution, i.e. the alternatives will be ranked with respect to the decreasing value of C_i^- from best to worst. According to the closeness index, A_1 which stands for ^{3}H source with the value of 0.58 is the best alternative and ^{63}Ni is the second priority and at last ^{14}C is the worst one considering the three criteria and their linguistic variables (Table 12).

Conclusion

In conclusion, analysis of simulation and analytical results using fuzzy TOPSIS method has proved that ^{3}H is the best alternative, considering important factors such as sensitivity, precision and saturation thickness. Also, other parameters such as 'spacing', 'detector type and dimension' and 'geometry factor' that define the

absolute efficiency of the system and the 'half-life' and the 'maximum energy emission' of the radioisotope that specify the effective lifetime of the gauge should be considered in advanced validations. Results have shown to be in an acceptable criteria, but prior to experimental tests, the spatial positions and spacing of the detector, source and substrates should be considered carefully.

References

1. Berry, R. W., Hall, P. M., & Harris, M. T. (1968). *Thin film technology*. New York: VanNostrand Reinhold.
2. Hurman, R. W. (1975). U.S. Patent No. 3,988,582A. Nucleonic Data Systems, Inc.
3. International Atomic Energy Agency. (2005). *Technical data on nucleonic gauges*. Vienna: IAEA. (IAEA--TECDOC-1459).
4. BAL SEAL Engineering (2003). *Metal plating processes and methods of measuring surface hardness and thickness coatings*. Amsterdam: Bal Seal Engineering. (TR-105).
5. Pocock, B. W. (1956). Application of beta-ray backscatter thickness gauge to traffic paint wear studies. In 2nd Pacific Area National Meeting of American Society for Testing Materials.
6. Dakota Ultrasonics. (2008). *Mmx-6 dl multi-mode ultrasonic thickness-meters*. *Operational Manual*.
7. Jaselskis, E. J., & Cackler, E. T. (2006). *Using laser for real--time pavement thickness measurement*. National Concrete Pavement Technology Center. (IHRB Project TR-538).
8. Kiang, G. C., & Lee, L. (1969). Study of the coating thickness measurement by the method of filtering backscattered beta particles. *Chinese J. Phys*., *7*(1), 2–8.
9. Wang, Y. J., & Lee, S. H. (2007). Generalizing TOPSIS for fuzzy multiple-criteria group decision-making. *Comput. Math. Appl.*, *53*, 1762–1772.
10. Hwang, C. L., & Yoon, K. L. (1981). *Multiple attribute decision making. Methods and application*. New York: Springer.
11. Katz, L., & Penfold, A. S. (1952). Range-energy relations for electrons and the determination of beta-ray end-point energies by absorption. *Rev. Mod. Phys*., *24*, 28–44.
12. Lapp, K. E., & Andrews, H. L. (1948). *Nuclear radiation physics*. New York: Prentice-Hall Inc.
13. Sharma, K. K., & Singh, M. (1980). Z-dependence of thick target β-ray backscattering. *J. Appl. Phys*., *51*, 2239–2243.
14. Cember, H., & Johnson, T. E. (2009). *Introduction to health physics* (4th ed.). New York: McGraw-Hill Medical.
15. Mahajan, C. S. (2012). Mass attenuation coefficients of beta particles in elements. *Science Research Reporter*, *2*(2), 135–141.
16. Thummel, H. W. (1974). Durschgang von elektronen und betastrahlung durch materieschichten. Berlin: Akademie--Verlag.
17. Sharma, K. K., & Singh, M. (1979). Variation of beta-ray backscattering with target thickness. *J. Appl. Phys*., *50*, 1529–1534.
18. Everhart, T. E. (1960). Simple theory concerning the reflection of electrons from solids. *J. Appl. Phys*., *31*, 1483–1490.
19. Archard, G. D. (1961). Back scattering of electrons. *J. Appl. Phys*., *32*, 1505–1510.
20. Briesmeister, J. F. (2000). *MCNP – A general Monte Carlo N-particle transport code.* (Version 4C). Los Alamos, NM: Los Alamos National Laboratory. (LA-13709-M).
21. Frujinoiu, C., & Brey, R. R. (2001). A Monte Carlo investigation on electron backscattering. *Radiat. Prot. Dosim*., *97*, 223–229.
22. Saremi, M., Mousavi, S. F., & Sanayei, A. (2009). *TQM consultant in SMEs with TOPSIS under fuzzy environment*. (Vol. 36, pp. 2742–2749).
23. Zadeh, L. A. (1965). Fuzzy sets. *Inform. Control*, *8*, 333–353.
24. Zimmermann, H. J. (1991). *Fuzzy sets theory and its application*. Dordrecht: Kluwer Academic Press.
25. Deng, H., Yeh, C. H., & Willis R. J. (2000). Inter-company comparison using modified TOPSIS with objective weights. *Comput. Oper. Res.*, *27*, 963–973.